16th Australasian Wind Engineering Society Workshop
Brisbane, Australia
18-19 July, 2013

Wind Loading Tributaries for Pierced Fixed Metal Roof Cladding

A.C. Lovisa[1], D.J. Henderson[2], V.Z. Wang[3] and J.D. Ginger[4]

[1]Ph.D. Research Scholar, School of Engineering,
James Cook University, Townsville, Australia

[2]Director, Cyclone Testing Station,
James Cook University, Townsville, Australia

[3]Lecturer, School of Engineering,
James Cook University, Townsville, Australia

[4]Associate Professor, School of Engineering,
James Cook University, Townsville, Australia

Abstract

Steel roof cladding is subjected to severe suction pressures during wind storms such as cyclones. These suction pressures, which are generated by the turbulent interaction of the wind flow around the building, vary both spatially and temporally. Extreme suction pressures can result in either static pull-through or fatigue failure of the roof cladding at its fixings. Given the complex nature of the pressures acting across the roof envelope, it is difficult to recreate these conditions during controlled experiments. Current testing methods for cladding and its fixings rely on the application of spatially uniform pressures to simulate cyclonic loading conditions, where only the effects of the temporal variations in pressure are included. This paper utilizes a validated numerical model to determine the effective tributary area of a fastener for corrugated roof cladding, in an attempt to establish whether a spatially uniform pressure is an adequate simplification. Experimental studies by Henderson and Ginger (2011) have similarly investigated the tributary area of a fastener using influence coefficients. The numerical model was used to recreate their experimental investigation and extends the investigation by studying the effects that the global response of the roof cladding has on the local response of the cladding at a fastener.

Introduction

The approach wind flow and its interaction with a low rise building generates fluctuating pressures across the roof envelope. The wind flow separates at the windward roof edge with reattachment taking place at various regions downwind on the roof, creating large spatial variations in applied pressure across the roof envelope. In regions of flow separation, such as the roof edges, cladding experiences highly fluctuating peak suction pressures due to the formation of vortices. These vortices result in dense spatial variations of pressure. For regions of flow separation, Surry *et al.* (2007) documented that the spatially averaged pressure across a 2.4 m by 4.3 m panel was a fifth of the magnitude of the peak suction pressure experienced by that same panel. In addition to spatial variations, the suction pressures acting on roof cladding fluctuate significantly, where several unique cycles can occur within a single second (Surry *et al.* 2007).

The severe suction pressures applied to roof cladding during wind storms such as cyclones can result in static pull-through failure or fatigue failure of the cladding at its fixings. Static pull-through failure occurs when a peak suction pressure forms a deep draw down of the fastener with radial splitting of the fastener hole. Fatigue failure is the more common mode of failure and is a result of the fluctuations in applied pressure (Morgan and Beck, 1977). The repeated loading of the fluctuating pressure generates fatigue cracking in the vicinity of the fasteners. These cracks continue to propagate and form a sizeable hole that then allows the fastener head to pull through.

Current design standards are reliant on experimental testing to measure the performance of cladding. For example, to determine the fatigue strength of the cladding, a specimen is installed within an air-box and a spatially uniform pressure of varying magnitude is applied to the cladding sheet for a specific number of cycles (Australian Building Codes Board, 2007). Only recently have realistic *temporal* variation in applied pressure been recreated experimentally using a pressure load actuator (PLA) (Henderson and Ginger, 2011).

Attempts have been made to apply both temporally *and* spatially varying pressures in experimental simulations, the most prominent example being the "Three Little Pigs" Project for the Insurance Research Lab for Better Homes of the University of Western Ontario. The "Three Little Pigs" project utilizes over 100 PLAs in combination with airbags to recreate the spatial and temporal variations in applied pressure across a full scale house (Kopp *et al.* 2010). However, replicating this project for standard testing of roof cladding is not viable and the application of a spatially uniform pressure is far more feasible. But is this an acceptable simplification for standard testing?

This paper investigates the tributary area of a cladding fastener using a numerical model. Once the tributary area of a fastener is known, the effects of spatial-averaging on the characterisation of the peak pressure can be measured. The studies undertaken by Henderson and Ginger (2011), who used influence coefficients to characterize the tributary area of a fastener, have been recreated using a numerical model of roof cladding. The model was then used to investigate the local response of the roof cladding when subject to a surface pressure across a whole cladding sheet and when subject to a localized pressure across the tributary of a fastener only.

Tributary Area of a Cladding Fastener for the Elastic Response

The limiting condition affecting both the static pull through strength and the fatigue strength of roof cladding is the fastener reaction load (Mahendran, 1990a; 1990b). The uplift load acting at a fastener can be calculated by Equation 1; where $I(x,y)$ is the influence coefficient for the uplift pressure, $p(x,y,t)$ is the uplift pressure acting on the cladding at (x,y) from the fastener, and dA is the area over which p acts.

$$F_z(t) = \int p(x,y,t) I(x,y) dA \quad (1)$$

Henderson and Ginger (2011) calculated the influence coefficient for corrugated roof cladding through experimental studies. Two G550 corrugated cladding sheets of 0.42 base metal thickness (bmt) were lapped together at the longitudinal edge as shown in Figure 1. A double-span configuration was favoured as it effectively simulates the in situ behaviour of cladding (Beck and Stevens, 1979). A series of point loads were applied to the cladding sheets at various locations along a fixed crest line while the resulting fastener reaction at a single fastener, known as the primary fastener, was recoded using a standard S-type load cell. The influence coefficient ($I(x,y)$) was then defined as the ratio of the fastener reaction load at the primary fastener (F_z) to the applied load at each location (x,y). Point loads were applied to both spans, along the primary crest line and the two adjacent crest lines; one of the adjacent crest lines was the lapped crest that joins the two cladding sheets.

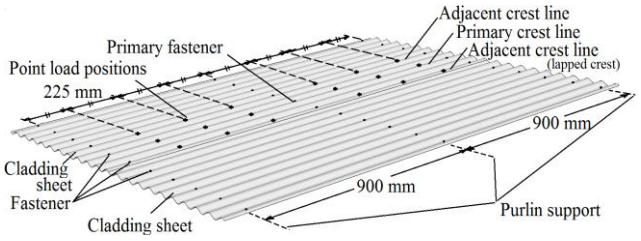

Figure 1. Experimental set-up used by Henderson and Ginger (2011)

A validated numerical model that can predict the static response of roof cladding was used to recreate the experiment undertaken by Henderson and Ginger (2011). The model was created by Lovisa *et al.* (2012) and is capable of predicting the fastener reaction at local plastic collapse with an accuracy of 96%. The model included only a single cladding sheet in order to simplify the simulation and subsequently reduce the simulation run time. As a result, the primary crest line and adjacent crest lines for the numerical model differ to that specified by Henderson and Ginger (2011) and are defined in Figure 2. The model applied point loads to the cladding sheet at the same positions along each crest line used by Henderson and Ginger (2011).

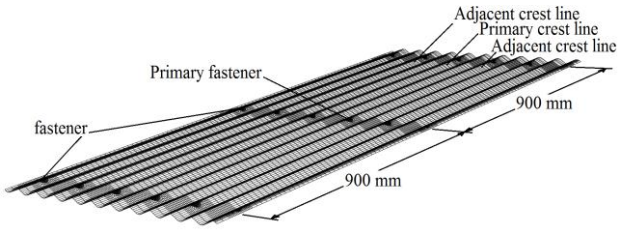

Figure 2. Numerical model of cladding sheet

The numerical model produced similar results to those documented by Henderson and Ginger (2011) with the tributary area elongated in the longitudinal direction. The fixed crest lines transfer the majority of the applied load, with approximately 5% of the load shedding to the adjacent fasteners. Figure 3 compares the numerical results with those documented by Henderson and Ginger (2011), and shows good agreement between the numerical and experimental results. Figure 3 also shows how the cladding behaves in a similar manner to a double span continuous beam, with the some plate action. Within the elastic response, the tributary area of corrugated cladding is an elongated area of 0.27 m^2 (152 mm fastener spacing × {2 × 900 mm span length}).

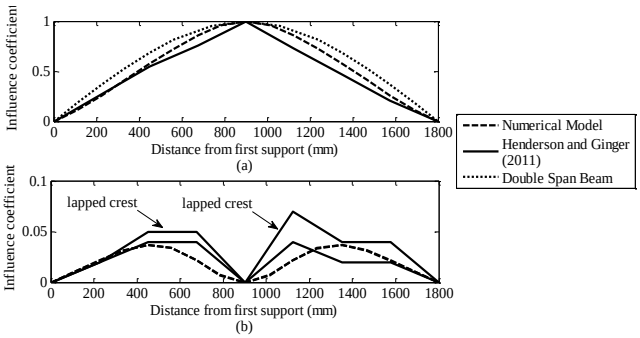

Figure 3. Theoretical, Numerical and experimental influence lines along (a) the primary crest line and (b) adjacent crest lines

Numerical Comparison of the Local Response of Roof Cladding Subject to Whole Surface and Localised Pressures

A numerical model can simulate a multitude of loading conditions that are too difficult to implement experimentally. The numerical model used to determine the influence coefficient of a cladding fastener has also been utilized for a direct comparison of the local response of the cladding when subjected to an uplift pressure across the entire cladding specimen and when subjected to a localised pressure across the tributary area only. A comparison of these two loading conditions will identify the extent of the effects that the global response of the cladding has on the local response. The first numerical simulation focused on the deflection, deformed shape and fastener reaction of a fixed crest at the centre support for a uniform uplift pressure applied to the entire cladding sheet, hereby referred to as the global model. The second numerical simulation again focused on the deflection, deformed shape and fastener reaction at the same fixed crest while a uniform uplift pressure was only applied to the tributary area of the fastener, hereby referred to as the local model. The local model was essentially a replica of the global model - the only the difference was the input loading conditions. The fastener in question and its relevant tributary area are indicated in Figure 4.

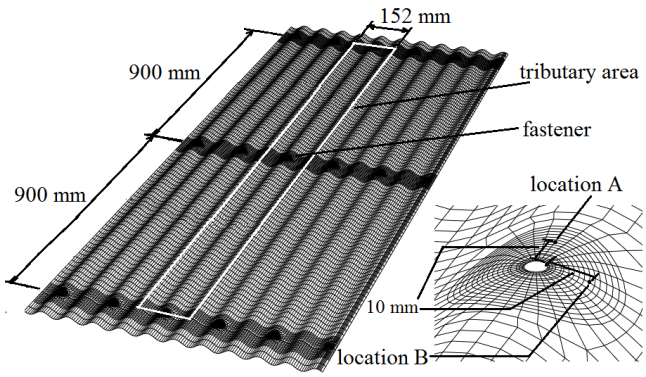

Figure 4. Numerical model for comparison of the local response of cladding subject to a pressure applied to the whole surface and a localised pressure applied to the tributary area only.

The fastener reaction predicted by both simulations is of particular importance as roof cladding experiences localized failure at the fastener by either dimpling, static pull-through or fatigue cracking; there is no global failure of the cladding sheet. Figure 5 compares the fastener reaction of a fastened crest at the centre support with the applied load for both the global and local model. The global model predicted that buckling would occur at a fastener reaction of approximately 770 N while the local model predicted buckling to occur at a fastener reaction of 725 N. The discrepancy between the two values is unusual given both models contain the same boundary conditions and material properties.

The global model may possess a stiffer profile in the transverse direction due to the large upward deflection of the unfixed crests. The reduction in the fastener reaction caused by the buckling of the cladding sheet also differed between loading conditions. The global model predicted that the fastener reaction would reduce by 80 N when the cladding buckled, whilst the fastener reaction described by the local model observed only a 30 N decrease.

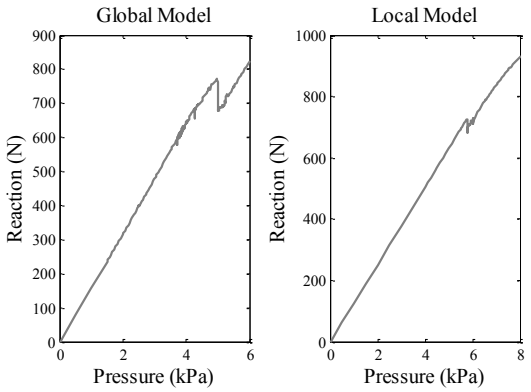

Figure 5. Fastener reaction for both numerical simulations

Of greatest interest is the applied pressure that results in buckling of the cladding. Figure 5 shows the global model buckling at an applied pressure of 5.0 kPa and the local model buckling at an applied pressure of 5.78 kPa. The similarity in result suggests the tributary area identified using influence lines is an effective representation of the true tributary area of a fastener.

The local response of the cladding can be described using deformation, or deflection, and stress across the cladding immediately adjacent to the fastener. Two points adjacent to the fastener were selected for a direct comparison of both stress and deflection. The two locations, known as locations A and B, are identified in Figure 4 and reside in the longitudinal and transverse directions. Both the transverse and longitudinal directions experience the principal stresses which causes cracking at the hole in both directions.

Figure 6 compares the reaction-deflection curves at locations A and B for both the global and local model. Plotting the deflection with respect to the fastener reaction was preferred given that both simulations performed consistently in terms of fastener reaction and could then be compared directly using fastener reaction. Clearly, the upward deflection predicted by both models is very similar at locations A and B.

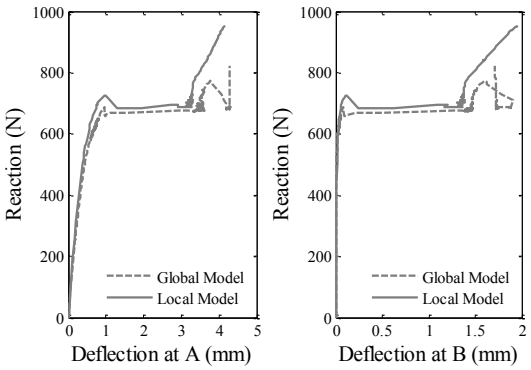

Figure 6. Reaction-deflection curve at locations A and B for both models

Although difficult to discern in the reaction-deflection curve, the global model predicted a two stage buckling process whilst the results from the local model has only a single distinguishable buckling stage. This two stage buckling process is, to an extent, evident in Figure 6 which shows the global model behaving differently to the local model after local plastic collapse.

Figure 7 describes the applied pressure-deflection curve for both models to highlight the two stage buckling process demonstrated by the global model. This two stage buckling process is an example of the global response affecting the local response. The first internal fixed crest in the global model buckled first, with each fixed crest then buckling sequentially. The initial flattening of an adjacent fixed crest (1st stage of buckling) resulted in a sudden increase in deflection at the fixed crest in question. As a result, the first stage of buckling occurred at an applied pressure of 4.3 kPa. However, the strain hardening characteristics of the material properties afforded reserve strength to the structure. Once the strain hardening was overcome by the applied load, the adjacent fixed crest would flatten further. The loss of stiffness at the adjacent crest caused a redistribution of the load, and the fixed crest in question would then buckle at an applied load of 5.0 kPa (2nd stage of buckling). This suggests the tributary area of a fastener changes once a fixed crest undergoes local plastic deformation (LPD). Figure 8 describes the deformed shape of the roof cladding at local plastic deformation.

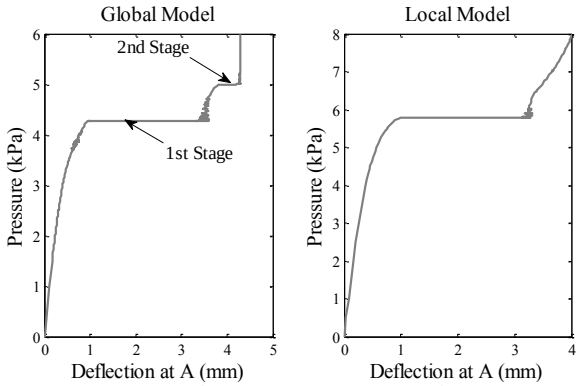

Figure 7. Pressure-deflection curve at location A for both models

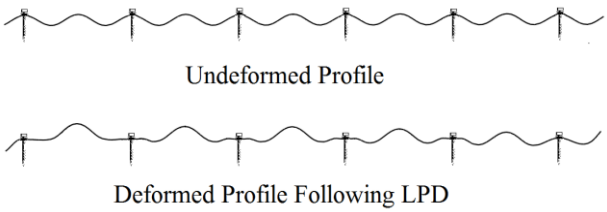

Figure 8. Local plastic deformation of corrugated roof cladding

The stresses in location A and B were also compared to characterise the local response of the roof cladding. At both locations A and B the cladding experiences a highly biaxial stress state. In order to perform a direct comparison between the global and local models, the Von Mises stress was used as it incorporates each component of stress. However, the Von Mises stress is usually preferred for determining the yield surface of isotropic materials only. The cladding described in both models is anisotropic. Nevertheless, the Von Mises stress was still used solely for comparative purposes since the yield strength of the cladding was not of interest. Figure 9 describes the Von Mises stress across the top surface of the cladding at locations A and B for both models. Both models predicted relatively similar magnitudes of stress. The complex changes in stress caused by buckling of the fixed crest were also similar for both models, excluding effects of the two stage buckling process predicted by the global model.

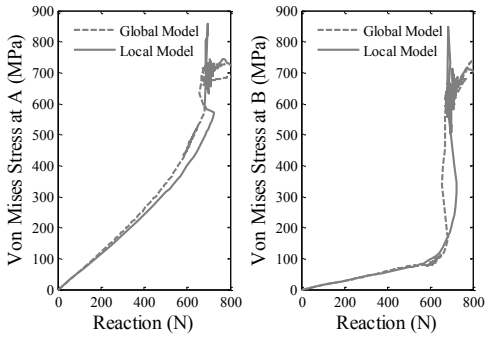

Figure 9. Von Mises stress at locations A and B for both models

Finally, the deformed shape of the cladding, in terms of the residual plastic deformation after unloading, was also used to characterise the local response of the cladding. The permanent plastic deformation of the cladding is a diamond shaped dimple and occurs when the cladding is loaded to, or beyond, local plastic deformation. Both models described a well-defined diamond shaped dimple following unloading, as demonstrated by Figure 10 (a) and (b).

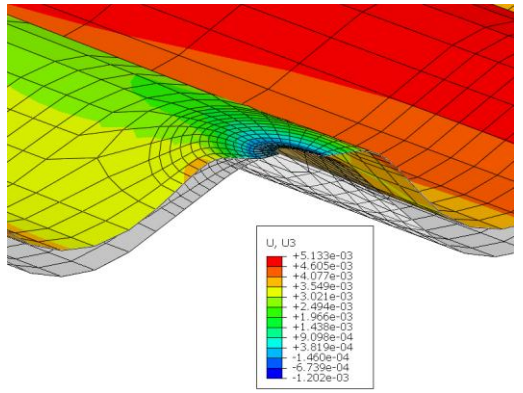

(a)

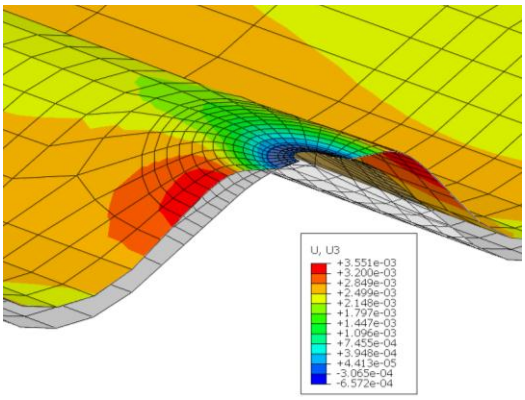

(b)

Figure 10. Permanent deformation of the cladding sheet following unloading for (a) the global model and (b) the local model.

An additional benefit of a numerical model is the ability to contour the entire model in terms of a variety of variables. One such variable is plastic strain. The local model was contoured with respect to plastic strain to determine the extent of the effects of applying a pressure to the tributary area of a fastener. Plastic strain was only found surrounding the fastener in question, with no plastic strain present at the adjacent fasteners.

Conclusion

Current testing methods used to measure the performance of roof cladding depend on the application of spatially uniform pressures. In situ roof cladding experiences both spatially and temporally varying pressures during a wind event. This paper investigated the effectiveness of simplifying the wind loading of roof cladding as a spatially uniform pressure. A numerical model was used to first investigate the extent of the tributary area of a cladding fastener using influence coefficients. The same model was then utilised to compare the local response of roof cladding when a pressure was applied to the whole surface of a cladding sheet and when a localised pressure was applied only to the tributary area of a fastener. Both analyses yielded the following conclusions:

- The tributary area of a fastener is elongated in the longitudinal direction, with 5% of the applied point load shed to the adjacent fastener. The tributary area of corrugated cladding specifically is an elongated area of 0.27 m^2 (152 mm fastener spacing × {2 × 900 mm span length}).
- The local response of the cladding is very similar when a uniform pressure is applied to the whole cladding sheet and when a localised pressure is only applied to the fastener tributary area. The global response of the cladding did affect the local response of the cladding at local plastic deformation only.
- A spatially uniform pressure is an adequate simplification of the complex wind loading conditions experienced by roof cladding.

References

Australian Building Codes Board. (2007). *BCA 2007: Building Code of Australia*. Canberra (ACT), Australian Building Codes Board

Beck, V. and Stevens, L. (1979). Wind loading failures of corrugated roof cladding. *Civil Engineering Transactions, IE Australia, 21*(1), 45-46.

Henderson, D. J. and Ginger J. D. (2011). Response of pierced fixed corrugated steel roofing systems subjected to wind loads. *Engineering Structures*, *33*(12), 3290-3298.

Jancauskas, E. D., Mahendran, M., & Walker, G. R. (1994). Computer simulation of the fatigue behaviour of roof cladding during the passage of a tropical cyclone. *Journal of Wind Engineering and Industrial Aerodynamics*, *51*, 215-227.

Kopp, G., Morrison, M., Gavanski, E., Henderson, D., and Hong, H. (2010). "Three Little Pigs Project: Hurricane Risk Mitigation by Integrated Wind Tunnel and Full-Scale Laboratory Tests". *Natural Hazards Review*, *11*(4), 151-161.

Lovisa, A.C., Wang, V.Z., Henderson, D.J. and Ginger, J.D. (2012). A finite element model for pierced-fixed, corrugated metal roof cladding subject to uplift wind loads. *Proceedings of the Australasian Structural Engineering Conference, Perth, Australia, July 2012*. Retrieved from: http://asec2012.conference.net.au/papers/037.pdf

Mahendran, M. (1990a). Fatigue behaviour of corrugated roofing under cyclic wind loading. *Civil Engineering Transactions, IE Australia*, *32*(4), 219-226.

Mahendran, M. (1990b). Static behaviour of corrugated roofing under simulated wind loading. *Civil Engineering Transactions, IE Australia, 32*(4), 211-218.

Morgan, J. W., & Beck, V. R. (1977). Failure of sheet-metal roofing under repeated wind loading. *Civil Engineering Transactions, I.E. Australia, 19*(1), 1-5.

Surry D., Sinno R., Nail B., Ho T., Farquhar S., Kopp G., (2007). "Structurally effective static wind loads for roof panels". *Journal of Structural Engineering – ASCE, 133*(6), 871-885.